Journal of proteome research

Article

pubs.acs.org/jpr

Quantitative Global Proteomics of Yeast PBP1 Deletion Mutants and Their Stress Responses Identifies Glucose Metabolism, Mitochondrial, and Stress Granule Changes

Gunnar Seidel,[†,§] David Meierhofer,[†,§] Nesli-Ece Şen,[‡] Anika Guenther,[†] Sylvia Krobitsch,[†,⊥] and Georg Auburger*[,‡,⊥]

[†]Max Planck Institute for Molecular Genetics, Ihnestraße 63-73, 14195 Berlin, Germany

[‡]Experimental Neurology, Goethe University Medical School, Theodor Stern Kai 7, 60590 Frankfurt am Main, Germany

Supporting Information

ABSTRACT: The yeast protein PBP1 is implicated in very diverse pathways. Intriguingly, its deletion mitigates the toxicity of human neurodegeneration factors. Here, we performed label-free quantitative global proteomics to identify crucial downstream factors, either without stress or under cell stress conditions (heat and NaN_3). Compared to the wildtype BY4741 strain, PBP1 deletion always triggered downregulation of the key bioenergetics enzyme KGD2 and the prion protein RNQ1 as well as upregulation of the leucine biosynthesis enzyme LEU1. Without stress, enrichment of stress response factors was consistently detected for both deletion mutants; upon stress, these factors were more pronounced. The selective analysis of components of stress granules and P-bodies revealed a prominent downregulation of GIS2. Our yeast data are in good agreement with a global proteomics and metabolomics publication that the PBP1 ortholog ATAXIN-2 (ATXN2) knockout (KO) in mouse results in mitochondrial deficits in leucine/fatty acid catabolism and bioenergetics, with an obesity phenotype. Furthermore, our data provide the completely novel insight that PBP1 mutations in stress periods involve GIS2, a plausible scenario in view of previous data that both PBP1 and GIS2 relocalize from ribosomes to stress granules, interact with poly(A)-binding protein in translation regulation and prevent mitochondrial precursor overaccumulation stress (mPOS). This may be relevant for human diseases like spinocerebellar ataxias, amyotrophic lateral sclerosis, and the metabolic syndrome.

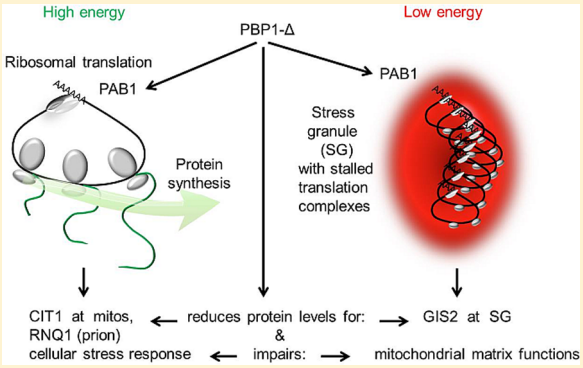

KEYWORDS: *PBP1, proteome profiling, mass spectrometry, stress response, neurobiology*

INTRODUCTION

An interestingly wide and diverse spectrum of molecular interactions and pathway roles was documented for the protein PBP1 in *Saccharomyces cerevisiae*, but its detailed function remains enigmatic. Both the deletion and the overexpression of PBP1 were shown to have beneficial effects in different contexts. Ten major observations exist on the function of PBP1.

(A) The deletion of PBP1 rescues the lethality resulting from deletions of PAB1 [poly(A)-binding protein], and it was demonstrated that PBP1 and PAB1 undergo direct protein−protein-interaction via the PAM2 motif within the ribosomal translation apparatus, which mediates the cosedimentation of PBP1 with polysomes and modulates the poly(A)-tail length of pre-mRNAs.[1] This protein interaction was conserved throughout phylogenesis until their mammalian orthologs ATXN2 and PABPC1.[2−6] However, the purpose of this translation modification and the identity of the regulated mRNAs still remains unclear. (B) The deletion of PBP1 rescues the growth defect resulting from double deletions of the cytoplasmic deadenylase CCR4 or the cytoplasmic deadenylase POP2 together with the RNA-binding protein KHD1, an effect that can also be achieved by deletions of the ribosomal large subunit proteins RPL12A and RPL12B.[7] (C) PBP1 also binds noncoding RNA, suppresses RNA-DNA hybrids, and prevents aberrant rDNA recombination. However, these benefits of PBP1 ablation bear the cost of a reduced replicative lifespan.[8]

Conversely, (D) the overexpression of PBP1 rescues mutants in the mitochondrial inner membrane protein TIM18, which are otherwise unable to live in the absence of mitochondrial DNA.[6,9] (E) In addition, the increased dosage of PBP1 rescues stress and cell death resulting from a loss of the mitochondrial proton gradient with subsequent cytosolic overaccumulation of mitochondria-targeted precursor proteins (mPOS), in parallel with the gain-of-function of several components of mRNA/ribosome/translation and mTOR signaling pathways.[10] (F) Interestingly, the ectopic overexpression of PBP1 in unstressed cells may mediate the sequestration of the kinase TORC1 into

Received: July 13, 2016
Published: December 14, 2016

DOI: 10.1021/acs.jproteome.6b00647
J. Proteome Res. 2017, 16, 504−515

stress granules during heat stress and the subsequent blunting of its growth signaling. This TORC1 sequestration is activated through phosphorylation of PBP1 by a kinase cascade involving the AMP-kinase ortholog SNF1 as well as PSK1.[11,12] Thus, the overactivity of PBP1 rescues mitochondrial dysfunction during cellular stress periods, (G) although PBP1 is exclusively localized at cytosolic stress granules (SG) together with its interactors PBP4 and LSM12 when bioenergetics reserves become low, but also these benefits come at the price of a limited growth of yeast colonies during PBP1 overexpression.[13]

Additional molecular insights into the mechanisms of PBP1 function were made, but most implicated proteins are poorly understood and not conserved through phylogenesis. (H) PBP1 associates with itself in a homodimer and with another PAB1-interactor named PBP4, also with the mRNA 3′-processing factors PIP1/PIP3, and with the signaling factor DIG1. Furthermore, PBP1 acts as negative regulator of poly(A) nuclease activity.[14] (I) PBP1 protein association with MKT1 modulates the mRNA translation of the endonuclease HO.[15] A joint conclusion from these observations might state that PBP1 acts as a stress response factor. Its role in stress periods must involve target molecules that are conserved throughout phylogeny but are unknown at present. Moreover, the identification of downstream factors has to be followed by the analysis of their involvement in pathology and phenotypes from yeast to human.

(J) Most intriguingly, the ablation of PBP1 mitigates the toxicity of human neurodegeneration protein TDP-43,[16] a nuclear RNA splicing and processing factor that appears in cytosolic ribonucleoprotein (RNP) granules in degenerating and stressed cells.[17−19] Deficiency of the ortholog of PBP1 in *Drosophila melanogaster* flies, named dATX2, was also shown to rescue the toxicity of various human neurodegenerative disease proteins. Beyond the rescue of TDP-43 toxicity, the deficiency of dATX2 also compensated the overexpression neurotoxicity of polyglutamine-domain expanded ATAXIN-1 and of polyglutamine-domain expanded ATAXIN-3.[16,20] Conversely, the overexpression of dATX2 hastened the neurodegeneration in mutants of ATAXIN-1, of ATAXIN-3, and of the microtubule associated protein TAU, which are known to display TOR-mediated growth activation.[20−24] A database that documents which human neurodegeneration disorders are subject to genetic modulation in *D. melanogaster*, *C. elegans*, and *S. cerevisiae*, has come to conclude that the PBP1 ortholog in human, named ATAXIN-2 (ATXN2), is a generic modifier that affects multiple if not all neurodegenerative diseases, similar to the antiapoptotic protein THREAD, the chaperone DNAJ-1, and the RNA-binding protein MUB.[25] In spite of the large therapeutic potential of the above-mentioned fly dATX2 modifier effects, again their molecular mechanisms remain to be defined.

In mouse and man, ATAXIN-2 is normally localized to the rough endoplasmic reticulum,[26] and its deficiency decreases the mRNA translation rate.[4] A minor part of ATAXIN-2 is also present at the plasma membrane in association with the growth factor receptor endocytosis complex, where the knockout of ATAXIN-2 leads to increased internalization of EGFR and decreases the levels of GRB2 and SRC kinase.[27−29] Human genome-wide association studies of genetic variants with the risk for diabetes mellitus type 1 and hypertension documented a role of the gene locus of *ATXN2* in multiple independent studies.[30]

In periods of cell stress, the mammalian ATAXIN-2 protein together with the poly(A)-binding protein PABPC1 relocalizes to stress granules, where RNA quality control takes place. It is important to note that the absence of ATXN2 was reported to prevent the formation of stress granules, while the overexpression of ATXN2 interferes with the formation of P-bodies where RNA decay occurs.[31]

The genetic ablation of ATXN2 in mouse leads to glycogen and lipid droplet accumulation with a progressive phenotype of insulin resistance and obesity.[32] Recent quantitative global proteome and metabolome studies of *Atxn2*-knockout liver and cerebellum documented severe reductions of mitochondrial enzymes involved in the degradation of fatty acid and branched amino acids (leucine, isoleucine, and valine), with concomitant changes also in the citrate cycle.[33] The most strongly downregulated mitochondrial enzyme (10-fold) of these pathways, Isovaleryl-CoA-dehydrogenase as a crucial enzyme of leucine metabolism and mTOR signaling, also exhibited a significant reduction of its transcript levels.[34] However, concerns were voiced that these dysregulations of ACAD (Acyl CoA dehydrogenase) enzymes might be due to positional effects, given that *ACAD10* is a neighbor gene of *ATXN2* and that homologous recombination events may alter the expression of neighboring genes within three mega bases distance.[35]

Thus, both the yeast PBP1 protein and its mammalian ortholog ATXN2 are implicated in growth pathways, nutrient metabolism, and bioenergetics, but the molecular mechanisms are not understood, particularly during cell stress.

Yeast cells can easily be subjected to stress and have limited complexity of the global proteome, so we explored their use for global expression profiling. In addition, the neighbor genes of *PBP1* are different from the *ATXN2* neighbor genes, so no ACAD enzyme is encoded in the vicinity, and it is possible to test whether a translation regulator such as PBP1 and its ortholog ATXN2 are indeed responsible for strong mitochondrial and bioenergetics adaptations to stress. Thus, an unbiased survey of the molecular consequences of PBP1 deficiency was attempted to exploit these advantages of yeast. In this approach, particular attention was paid to understand the role of PBP1 for stress granule and P-body components. To reduce false-positive results through consistency filters, two haploid yeast strains with complete PBP1 deletions were used, and two stress conditions were applied. Heat and also the respiration inhibitor NaN_3 were previously shown to trigger stress granule formation in yeast.[11,36] Global proteome abundance was quantified with label-free mass spectrometry and consistent changes beyond 1.5-fold were selected. This threshold was chosen in view of chromosomal trisomy and gene duplication events that result in a 1.5-fold gain-of-function and trigger frequent age-associated neurodegenerative disorders like Down syndrome, Alzheimer's disease, and Parkinson's disease in human.[37−39] Protein interactions and pathway effects were studied with bioinformatic tools.

The results indicated a prominent modulation of stress pathways in unstressed cells. During stress periods, a modulation of glucose and mitochondrial metabolism as well as an influence on GIS2 was apparent. GIS2, a ribosomal translation modifier of mitochondrial precursor protein synthesis in periods of reduced mitochondrial import, represented a central node among the protein−protein-interaction network of dysregulated factors within stressed PBP1-deleted cells.

DOI: 10.1021/acs.jproteome.6b00647
J. Proteome Res. 2017, 16, 504−515

EXPERIMENTAL PROCEDURES

Yeast Strains and Stress Conditions

The wildtype strain BY4741 (MATa; ura3Δ0; leu2Δ0; his3Δ1; met15Δ0) (abbreviated BY in this manuscript), which was used as reference strain, was purchased from the EUROSCARF (European *Saccharomyces cerevisiae* archive for functional analysis) collection center. This strain was originally derived from *S. cerevisiae* strain S288C as described previously.[40]

In addition, one of the used PBP1 deletion strains was also obtained from EUROSCARF. Therefore, we coined this strain ΔPBP1-deletion bank (DB) to distinguish it from a second PBP1 deletion strain used in this study (see below). The DB strain (MATa; ura3Δ0; leu2Δ0; his3Δ1; met15Δ0; YGR178c::kanMX4) was created as part of the EUROFANII (European project for the functional analysis of unknown genes II), which aimed at the systematic depletion of *S. cerevisiae* genes. According to the guidelines of this project, DB was derived from BY4741 via homologous recombination of a heterologous KanMX4 gene deletion cassette into the PBP1-ORF on yeast chromosome 7, using PCR-amplified oligonucleotides, as exemplified.[41] Furthermore, every yeast-KO strain was labeled with unique Tag-sequences up- and downstream of the inserted deletion cassette, which were used by us to validate the PBP1-deletion via sequencing.

The second PBP1-deletion strain on the other hand was created and designated ΔPBP1-self-made (SM). This strain was made akin to the DB strain using an amplified loxP-KanMX4-loxP deletion cassette, which was coupled to a 42 bp region homologous to a sequence upstream of the PBP1-ORF on the 5′-end and a 37 bp region homologous to a sequence downstream of the ORF on the 3′-end. The respective primer sequences were 5′-CTGACATCCTCAGTCACGGAAGTAATTAAAGGAGTTCATTACGTACGC-TGCAGGTCGACAAC-3′ (sense) and 5′-GTACCACTGATTATATACCATATTTATAAAGTGCAT-GGTGAGCGAGGAAGCGGAAGA-3′ (antisense), and the reaction was performed with the pUG6-plasmid as a template according to an established protocol.[42] The obtained amplicon was then transformed into yeast strain BY4741 for homologous recombination and the transformation mixtures were plated on G418 containing agar plates to select for KanMX4 bearing clones. Those were then transformed with the plasmid pSH47 encoding Cre-recombinase to excise the deletion cassette at its LoxP-sites and subsequently selected on 5-FOA-plates to eliminate the pSH47 plasmid. Finally the remaining insert sequence was PCR-amplified using the primers 5′-GAGTTCAATGTAGCCTGAGA-3′ (sense) and 5′-GATATAGGTCATTCACTCGC-3′ (antisense), and the amplicon's sequence was determined. After all, the sequencing confirmed the successful deletion of PBP1 in the SM strain.

The strains were grown in YPD + 2% glucose medium to a final OD600 of 0.7. Cells were harvested by centrifugation for 5 min at 4000 × *g* at 4 °C. For stress administration, resuspension of the cells in YPD + 2% glucose medium preheated to 46 °C heat for 15 min or containing 0.5% sodium azide/NaN_3 for 30 min was performed before protein extraction, as established means to trigger stress granule formation.[36,43]

Sample Preparation for Yeast Proteome Profiling

Yeast samples, as biological triplicates for every strain and condition, were prepared as described[44] and were lysed in a buffer containing 8 M Urea, 50 mM Tris, 75 mM NaCl with proteinase inhibitors and solubilized with glass beads. Protein concentration was measured with Bradford. Same protein amounts were reduced by dithiothreitol and alkylated by chloroacetamide. Tryptic digest was performed in a dilution to 1.5 M urea with 50 mM Tris, pH 8.0 with an enzyme to protein ratio of 1:50 at 37 °C, ON. An additional 1:50 ratio was added the next day for 1 h. The digests were quenched by addition of formic acid to a final concentration of 1%, desalt by C18 tips (Pierce). Eluates were lyophilized, dissolved in 5% acetonitrile, and 2% formic acid for subsequent LC−MS analysis.

LC−MS Settings for Proteomics

LC−MS/MS was carried out by nanoflow reverse-phase liquid chromatography (Dionex Ultimate 3000, Thermo Scientific, USA) coupled online to a Q-Exactive Plus Orbitrap mass spectrometer (Thermo Scientific) as described previously by us.[33] Briefly, LC separation was performed using a PicoFrit analytical column (75 μm ID × 40 cm long, 15 μm Tip ID (New Objectives, Woburn, MA, USA)) in-house packed with 2.1-μm C18 resin (Reprosil-AQ Pur, Dr. Maisch, Germany). Peptides were eluted using a gradient from 3.8 to 98% solvent B over 192 min at a flow rate of 266 nL/min (solvent A: 0.1% formic acid in water; solvent B: 80% acetonitrile and 0.08% formic acid). For nanoelectrospray generation, 3.5 kilovolts were applied. A cycle of one full FT scan mass spectrum (300−1750 m/z, resolution of 70 000 at m/z 200, AGC target $1e^6$) was followed by 12 data-dependent MS/MS scans (200−2000 m/z, resolution of 35 000, AGC target $5e^5$, isolation window 2 m/z) with normalized collision energy of 25 eV. Target ions already selected for MS/MS were dynamically excluded for 30 s. In addition, only peptide charge states between two to eight were allowed.

Proteomics Data Analysis and Statistics

Raw MS data were processed with MaxQuant (v1.5.3.30)[45] with the Andromeda search engine[46] and searched against *Saccharomyces cerevisiae* (yeast) with 6.741 entries, released in 2014−11. A false discovery rate (FDR) of 0.01 for proteins and peptides and a minimum peptide length of seven amino acids were required, a mass tolerance of 4.5 ppm for precursor and 20 ppm for fragment ions were required. A minimum Andromeda score of 0 and 40 (delta score 0 and 9) for unmodified peptides and modified peptides was applied. A maximum of two missed cleavages was allowed for the tryptic digest. Cysteine carbamidomethylation was set as fixed modification, whereas N-terminal protein acetylation and methionine oxidation were set as variable modifications. Contaminants as well as proteins identified by site modification and proteins derived from the reversed part of the decoy database were strictly excluded from further analysis.

The correlation analysis of biological replicates and the calculation of significantly different proteins were done with Perseus software (v1.5.2.6). LFQ intensities, originating from at least two different peptides per protein group, were log-transformed. Only protein groups with valid values within compared experiments were used for further data evaluation. The MaxQuant processed output files can be found in Supplemental Table S1, showing peptide and protein identification, accession numbers, % sequence coverage of the protein, q-values, and LFQ intensities. Statistical analysis was done by a two sample t test with Benjamini−Hochberg (BH, FDR of 0.05) correction for multiple testing. Significantly regulated proteins between experiments were indicated by a plus sign in Supplemental Table S2. The mass spectrometry data have been deposited to the ProteomeXchange Consortium

DOI: 10.1021/acs.jproteome.6b00647
J. Proteome Res. 2017, 16, 504−515

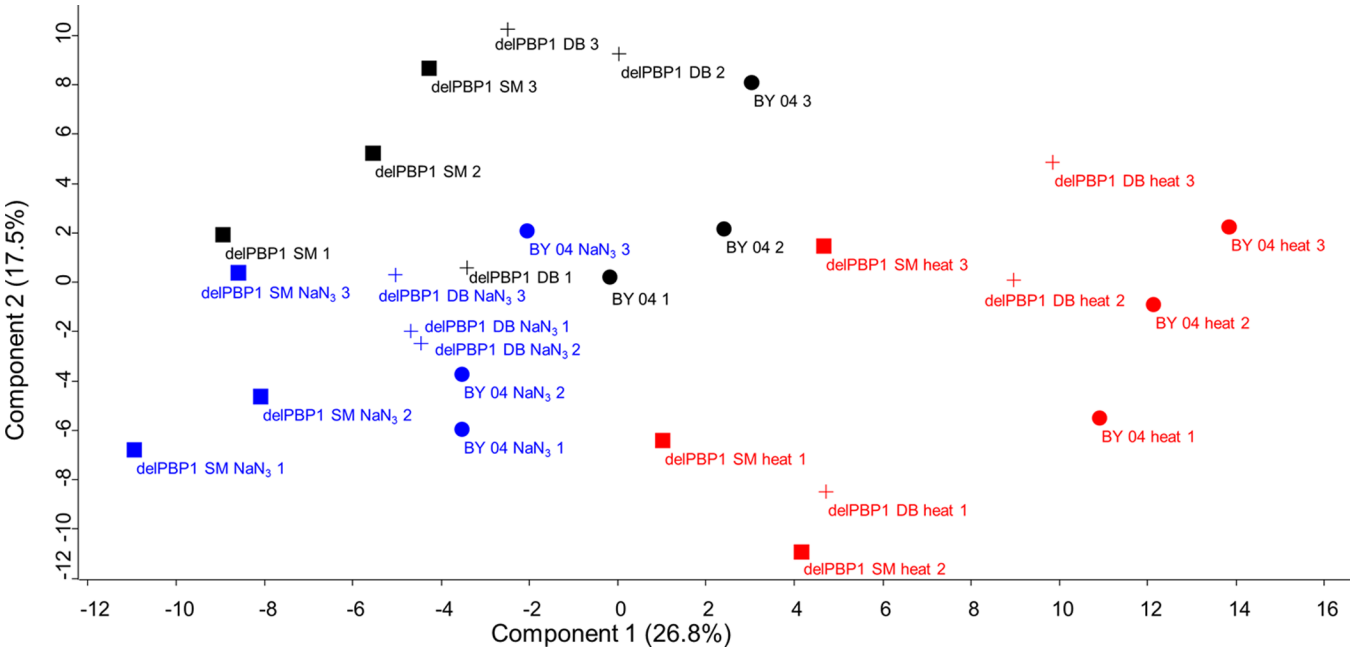

Figure 1. Principal component analysis of wildtype strain (BY4741) versus two mutant strains (SM and DB) and unstressed state versus two stress conditions (heat and NaN_3). The proteome data sets are represented by black letters in the case of unstressed strain replicates, by blue letters for NaN_3 stress conditions, and by red letters for heat stress conditions.

(http://proteomecentral.proteomexchange.org) via the PRIDE partner repository[47] with the data set identifier PXD003868.

Protein–Protein Interaction (PPI) Network Analysis

Proteins with a dysregulation effect size ≥1.5-fold (Supplemental Table S2) were used to generate PPI interaction networks using STRING v10 (Search Tool for the Retrieval of Interacting Genes)[48] by considering only experimental determined interactions with a medium confidence score of 0.4, and focusing primarily on the pathways defined by KEGG (Kyoto Encyclopedia of Genes and Genomes). The ≥1.5-fold cutoff has been chosen because the dosage effects of three gene copies instead of two gene copies result in age-associated neurodegenerative diseases, in the case of crucial factors like amyloid-precursor-protein or alpha-synuclein.[37−39]

Starvation Experiments

As previously described,[49] human SH-SY5Y neuroblastoma cells normally cultured in growth medium (RPMI 1640 containing 2 g/L D-glucose and 2 mM L-glutamine) were starved of trophic factors and nutrients by incubating them without FCS and in HBSS medium (low glucose 1 g/L and no amino acids) (Invitrogen). Always 20 h prior to stress, 0.5×10^6 SH-SY5Y cells were seeded in a six-well plate. At different time points after the medium change, specific transcript changes of 30 ng cDNA per sample were analyzed with the appropriate TaqMan gene expression assays (Applied Biosystems, Darmstadt, Germany): *ATXN2* (Hs00268077_m1), *CS* (Hs02574374_s1), *CNBP* (Hs00231535_m1), *PRNP* (Hs01920617_s1). The mean of expression changes was normalized to the mean of Hypoxanthine Phosphoribosyltransferase 1 (*HPRT1*: Hs99999909_m1) as an internal housekeeping gene control. Relative expression changes were calculated with the $2^{-\Delta\Delta Ct}$ method,[50] whereupon the ΔCt of the corresponding control served as a calibrator. The resulting $2^{-\Delta\Delta Ct}$ values of n experiments were averaged for each time point.

RESULTS

Global Proteome Quantification

To elucidate the molecular effects of PBP1 deletion in yeast during logarithmic growth, we performed global proteome quantification by label-free mass spectrometry. The genotype of the yeast strains was verified by sequence validation after amplification of either specific Tag-sequences or the empty PBP1-locus. In both deletion strains, the mass spectrometry data did not contain peptides of PBP1, whereas 85 peptides were identified in the other samples (data not shown).

Comparison of all 27 biological triplicates from wildtype BY strain and both PBP1 deletion strains (DB and SM), without stress and with heat as well as NaN_3 stress, was done by Pearson correlation, which revealed highly similar coefficients with a range of 0.902−0.987 (Supplemental Figure S1). These Pearson correlation coefficients indicated a very good quality of the proteome data sets. The entire list of identified and quantified protein groups can be found in Supplemental Table S1 and represents 3197 protein groups.

A principal component analysis in two dimensions (Figure 1) revealed that the heat stress dysregulated the proteome in a different direction and with stronger effect than the NaN_3 stress, with the PBP1 deletion apparently curbing the heat response in comparison to the wildtype strain.

The SM deletion strain in all conditions generated stronger dysregulations in similar direction compared to the DB deletion strain. The only known difference between the two PBP1 deletions strains lies in the fact that the DB strain obtained from the yeast deletion bank still contains the kanamycin resistance selection marker, while the freshly generated SM deletion strain had this selection marker removed by Cre-LoxP technology. So possibly the removal of the kanamycin resistance cassette altered the levels of the physiological oxidative stress in the cells. Thus, subsequent analyses were performed (1) using volcano plots as a very stringent tool to identify proteins with consistent dysregulations for both

DOI: 10.1021/acs.jproteome.6b00647
J. Proteome Res. 2017, 16, 504−515

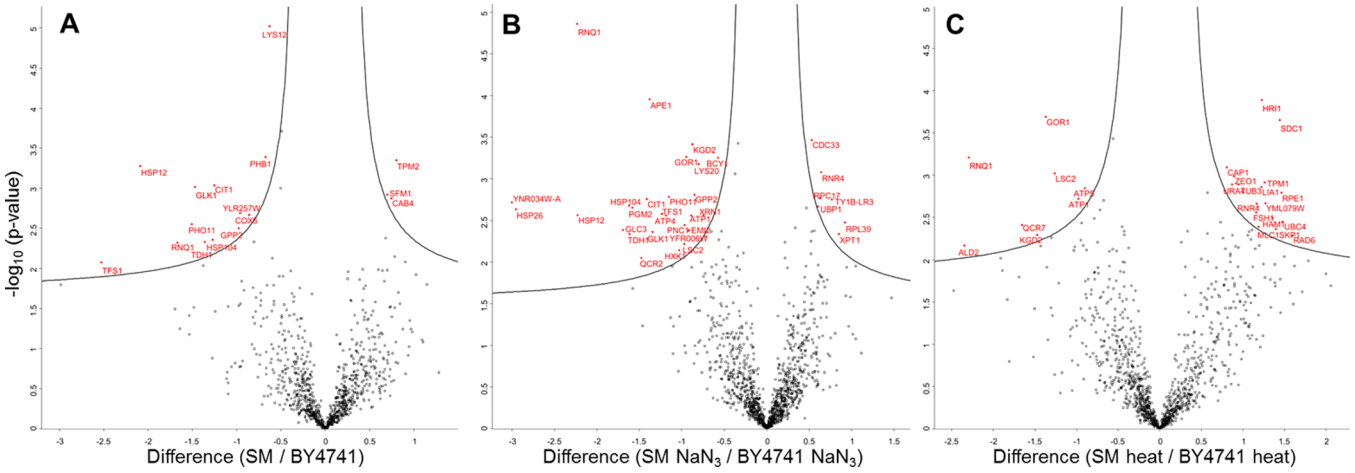

Figure 2. Volcano plots for (A) SM versus wildtype BY4741 without stress, (B) SM with NaN_3 versus wildtype BY4741 with NaN_3, (C) SM with heat versus wildtype BY4741 with heat. The indicated *p*-value cutoff is pre BH correction.

stressors, and (2) using a threshold of at least 1.5-fold effect size to identify proteins with consistent either up- or down-regulation in both deletion strains.

An initial survey of the data with volcano plots revealed significant results for the SM deletion mutant (Figure 2A–C), while no significant data were observed in volcano plot analysis for the DB mutant.

Only two proteins consistently showed significant down-regulations in all three volcano plots, namely the cytosolic yeast prion protein RNQ1 (−4.2-fold) and the mitochondrial citrate synthase CIT1 (−2.6-fold). One protein showed significant downregulation without stress and under NaN_3 stress, while missing significance barely under heat stress, the cytosolic glucokinase GLK1 (−2.4-fold). Exclusively under the two stress conditions, significant downregulations of the cytosolic hypoxia-responsive YNR034W-A (−4.5-fold),[51] the mitochondrial glyoxylate reductase GOR1 (−2.2-fold), the mitochondrial alpha-ketoglutarate dehydrogenase component KGD2 (−2.2-fold), the mitochondrial succinyl-CoA ligase subunit LSC2 (−2.2-fold), and the mitochondrial ATP synthase component ATP1 (−1.9-fold), as well as the upregulation of the cytosolic and nuclear DNA-damage response factor ribonucleotide-diphosphate reductase RNR4 (+1.9-fold), were observed with consistency. These data clearly reflect alterations of mitochondrial bioenergetics, cytosolic glucose utilization, and stress response factors.

Consistent Dysregulations with >1.5-Fold Effect Size

In a first step, three dysregulations were identified that occurred in all six comparisons, namely both PBP1 deletions strains without stress as well as under both stressors, and showed effect sizes beyond a cutoff value of 1.5-fold. These comprised consistent downregulations of the yeast prion protein RNQ1 (−3.9-fold) and the key bioenergetics enzyme KGD2 (−1.7-fold) as well as a consistent upregulation of the leucine biosynthesis enzyme LEU1 (+1.7-fold). The LEU1 dysregulation has to viewed with caution, given that the yeast strains adapted for laboratory use always have a deletion in the LEU2 gene, but of course the result was obtained by comparison with the appropriate wildtype yeast lab strain BY4741, and the deletion of the mammalian ortholog ATXN2 also leads to altered leucine metabolism.[52]

A consistent dysregulation in five among the six comparisons was documented for the cytosolic glycogen branching enzyme GLC3 (−2.4-fold), the cytosolic glycolysis/gluconeogenesis factor TDH1 (−2.3-fold), the mitochondrial citrate synthase CIT1 (−2.1-fold), the cytosolic heat shock protein HSP104 (−2.2-fold), the membrane pump and salt-stress tolerance factor ENA1 (+2.2-fold), the cytosolic proteasome regulator and nuclear DNA-damage repair factor RAD6 (+2.1-fold), and the cytosolic and nuclear methionine biosynthesis enzyme MRI1 (+1.8-fold).

In the absence of stress, the consistent dysregulation effects in both deletion mutants upon PPI analysis showed no enrichment among 22 upregulated factors, but significant enrichment among 17 downregulated factors (ATP14, ATX1, CIT1, DDR48, HSP104, HSP12, HSP150, HSP26, KGD2, MLP1, MRH1, RIM1, RNQ1, RPS30B, SSA4, TFS1, YDL124W), for the biological processes (GO term) cellular response to heat (FDR q = 3.1e−2), and cellular response to stress (FDR q = 4.1e−2) upon analysis with the STRING Web server.

In the presence of a cell stress, 161 factors showed a consistent dysregulation at least in the same mutant for both stressors or in both mutants for one stressor. A PPI network, including all downregulated proteins with a ≥ 1.5-fold regulation in SM and DB versus BY with both stressors, was created (Figure 3). The network shows cytosolic bioenergetics and stress response factors such as heat shock proteins on the lower left, a network of mitochondrial bioenergetics and metabolism factors on the upper left, as well as a prominent node of interactions with the stress granule component GIS2 on the right side (Figure 3). Interestingly, four out of seven known eisosome proteins were found to be reduced in the deletion strains (EIS1, LSP1, PIL1, YGR130C).

A KEGG pathway analysis within this PPI network and a Bonferroni cutoff ≤0.05 revealed oxidative phosphorylation, TCA cycle, and several amino acid metabolisms to be significantly downregulated under stress conditions (Table 1). In our previous study of the ortholog ATAXIN-2 in a mouse KO model, we observed very similar affected downregulated pathways.[52]

Overall, the analysis of 1.5-fold dysregulations, which were consistent between both PBP1 deletion mutants, confirmed the modulation of mitochondrial metabolism, cytosolic bioenergetics, and proteostasis that had been previously detected by Volcano plot analysis in the SM mutant.

DOI: 10.1021/acs.jproteome.6b00647
J. Proteome Res. 2017, 16, 504−515

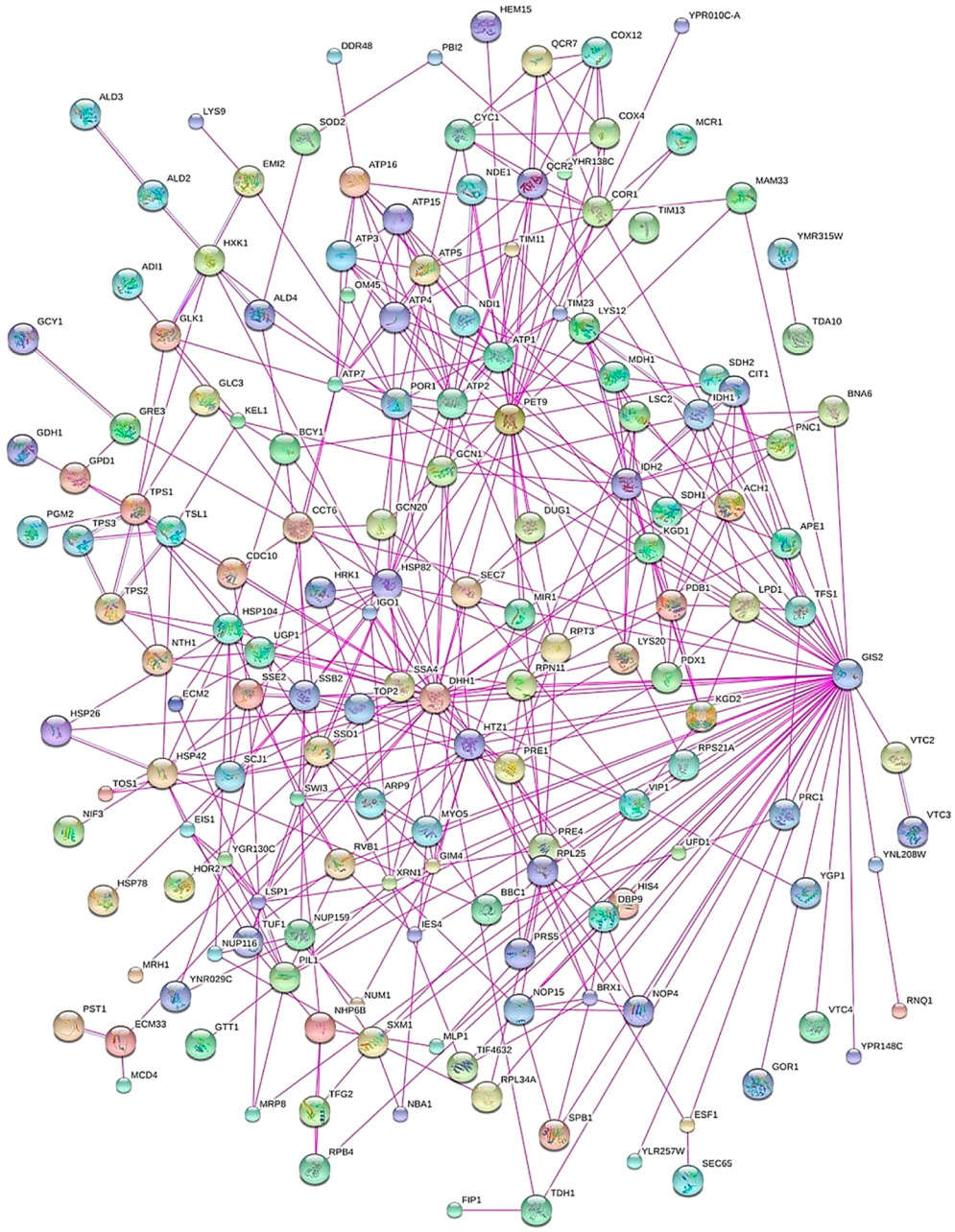

Figure 3. STRING PPI network analysis of ≥1.5-fold regulated proteins of SM + DB versus BY with both stressors. The red lines represent interactions that were experimentally determined. The coloring of the circles representing each protein is random, a predicted 3D-structure is shown inside the circle for each protein.

Systematic Evaluation of Stress Granule and P-Body Components

Given that PBP1 is relocalized to stress granules during cell stress periods, thus modulating RNA quality control in these RNP granules and also influencing the downstream RNA decay at P-bodies,[13] we investigated the effects of PBP1 deletion on the 36 known stress granule (SG) components and the 47 known P-body (PB) components in a systematic manner, as listed in the *Saccharomyces* genome database. In the absence of stress, the loss of PBP1 in both deletion strains reduced the abundance of the RNA-binding chaperone HSP26 (in DB to 44%, in SM to 14%) and of the mPOS factor GIS2 (in DB to 84%, in SM to 44%), a protein present both in SG and PB. At the same time, the PB component and putative ribophagy factor BRE5 was increased (in DB to 175%, in SM to 166%).

During NaN_3 stress, the RNA-binding chaperone HSP26 was significantly downregulated (in DB to 44%, in SM to 13%, Figure 4A) in both deletion mutants, while downregulations with significance only in the SM deletion mutant were observed for the mPOS regulator GIS2 (to 60%) and the 5′-3′ exonuclease XRN1 (to 59%).

During heat stress, a downregulation was noted to some degree for HSP26 (in DB to 90%, in SM to 63%), but prominently for GIS2 (in DB to 56%, in SM to 26%; Figure 4B) in concordance with the dysregulation of many of its putative interactors (Figure 3).

DOI: 10.1021/acs.jproteome.6b00647
J. Proteome Res. 2017, 16, 504−515

Table 1. KEGG Pathway Analysis within the PPI Network of ≥1.5-Fold Regulation in SM and DB versus BY with Both Stressors, As Visualized in Figure 3

KEGG pathway	number of genes	*p*-value	*p*-value Bonferroni
metabolic pathways	70	3.9×10^{-23}	4.18×10^{-21}
biosynthesis of secondary metabolites	35	1.5×10^{-14}	1.6×10^{-12}
microbial metabolism in diverse environments	23	1.21×10^{-10}	1.3×10^{-8}
oxidative phosphorylation	16	1.23×10^{-10}	1.31×10^{-8}
carbon metabolism	19	1.87×10^{-10}	$2{,}00 \times 10^{-8}$
citrate cycle (TCA cycle)	11	6.57×10^{-10}	7.03×10^{-8}
starch and sucrose metabolism	10	9.68×10^{-8}	1.04×10^{-5}
biosynthesis of amino acids	14	8.66×10^{-6}	9.26×10^{-4}
histidine metabolism	5	2.02×10^{-5}	2.16×10^{-3}
glycolysis/gluconeogenesis	9	2.31×10^{-5}	2.47×10^{-3}
pyruvate metabolism	7	3.36×10^{-5}	3.6×10^{-3}
beta-alanine metabolism	4	2.77×10^{-4}	2.96×10^{-2}
glyoxylate and dicarboxylate metabolism	5	3.34×10^{-4}	3.58×10^{-2}
lysine degradation	4	3.91×10^{-4}	4.18×10^{-2}

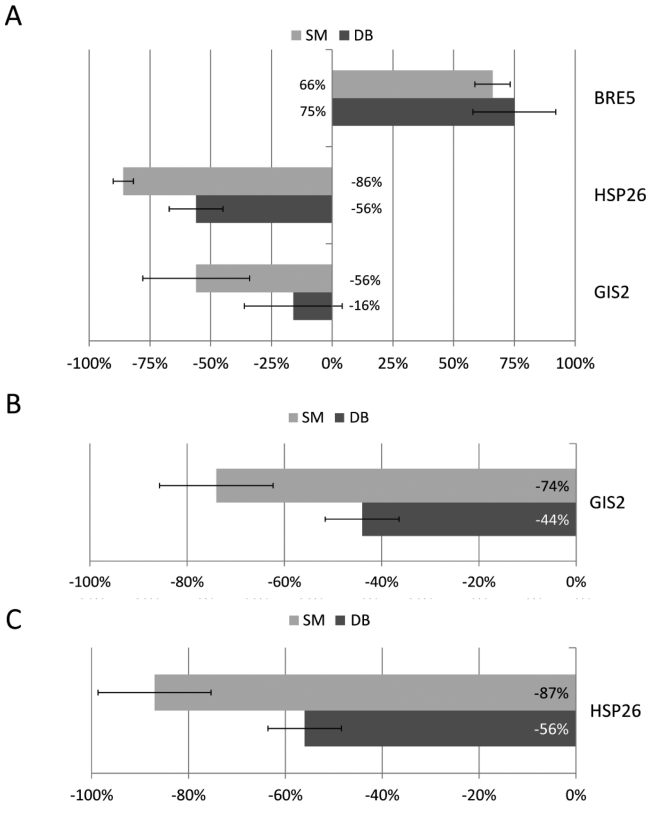

Figure 4. Stress granule and P-body components with >1.5-fold dysregulations in SM and DB strains. (A) Results of the comparison of two unstressed PBP1 deletion strains with the unstressed wildtype strain BY4741. (B, C) Results of the comparison of two stressed PBP1 deletion strains compared to the stressed wildtype strain BY4741 using either (B) NaN_3 stress or (C) heat shock as stressor (HSP26 and GIS2 can be part of P-bodies and stress granules, whereas BRE5 is only part of PB). Dysregulation percentage reflects the triplicate measurements, variance is shown as standard error of the means.

Overall, our conditions of heat stress more than NaN_3 stress elicited dysregulations of various SG components in dependence on PBP1 deletion, with the downregulation of GIS2 being the most consistent effect.

Validation of Similar Dysregulations in Human Neural Cells during Stress Conditions

Given that ATAXIN-2 has a role for the balance between obesity and atrophy in human disease and that it acts via the processing of specific mRNAs, we tested the relevance of our yeast data in man by quantitative real-time reverse transcriptase PCR (qPCR). We thus studied selected mRNA levels in human SH-SY5Y neuroblastoma cells carrying a stable lentiviral knockdown of ATAXIN-2 or a scramble control. This was performed in a time course analysis after starvation stress since ATAXIN-2 was recently shown to play a prominent role in calorie-restricted *C. elegans* worms.[53] This assay was previously found useful to understand the transcriptional regulation of key factors in the mitochondrial quality control during stress periods, namely of ATAXIN-2, PINK1, and PARKIN.[49,54−56] As shown in Figure 5, similar dysregulations in human cells as in yeast were observed in dependence on ATAXIN-2 deficiency for the mRNA levels of the prion membrane protein (*PRNP*), the mitochondrial bioenergetics enzyme citrate synthase (*CS*), and the human GIS2 ortholog at stress granules (*CNBP*). Thus, the documentation of the global proteome of yeast with PBP1 deletion during cell stress has generated insights that are relevant for human diseases.

DISCUSSION

The proteome profile of yeast PBP1-deficiency in the absence of stress is comparable with the previously published proteome profile of mouse *Atxn2*-KO tissues.[52] It clearly confirms that profound downregulations of key bioenergetics enzymes (in yeast KGD2, GLK1, COX6, TDH1, CIT1, ATP14, LYS12, GPP2; in mouse ACADS, ACAD9, ACAD8, ALDH6A1, ALDH7A1, PCCA, PCCB and several enzymes of the citric acid cycle) and of a key enzyme of leucine metabolism (in yeast LEU1; in mouse IVD, ACADM, ACAD2, MCCC1, MCCC2) are conserved throughout phylogeny. Of course, the LEU1 finding has to be considered with caution, given that lab yeast strains always have a LEU2 deletion. Definitely, the strong effect of PBP1 deletion on bioenergetics and mitochondrial proteins argues against the notion that the deletion of the translation modifier *Atxn2* affects mitochondrial factors only via interference with its neighbor gene *Acad10*. Furthermore, the *Acad10* transcript levels are unchanged by the *Atxn2*-KO mouse brain and liver (data not shown). On the contrary, the findings clearly substantiate the concept that both translation modulators PBP1/ATXN2 have a preferential impact on enzymes in the cytosolic bioenergetics pathways and in the mitochondrial metabolism. These proteome findings in yeast are also in excellent agreement with recent global transcriptome observations in mouse mutants and human SCA2 patients, that ATAXIN-2 modulates the mRNA levels of the mitochondrial stress response and quality control factor PINK1.[49] It is also consistent with a recent report that the ancestor of ATAXIN-2 and ATAXIN-2-like in *C. elegans*, ATX-2, controls cell size and fat content prominently in animals with nutrient restriction.[53] In addition, it provides an explanation why the deletion of ATAXIN-2 in mouse and genetic variants at the chromosomal locus of ATAXIN-2 in human populations trigger an obesity phenotype.[30,32]

Furthermore, the data confirm that the deletion of PBP1 even in the absence of stress reduces the levels of proteostasis

DOI: 10.1021/acs.jproteome.6b00647
J. Proteome Res. 2017, 16, 504−515

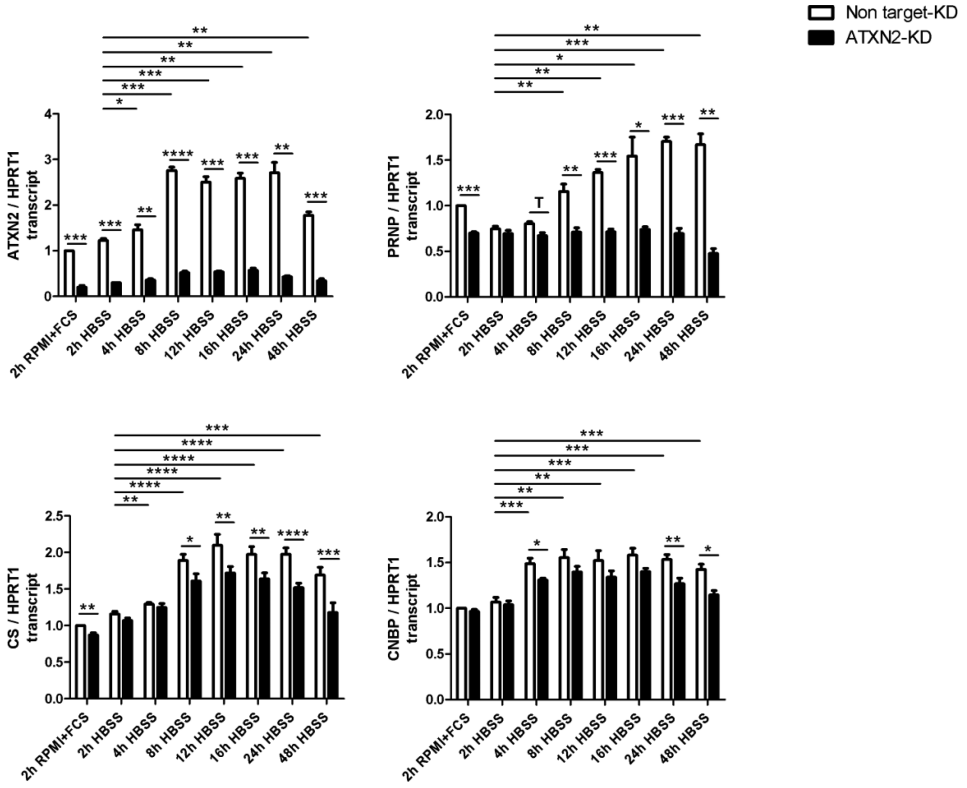

Figure 5. Validation of similar dysregulations in human neuroblastoma cells with stable ATAXIN-2 knockdown during starvation stress. Cells were cultured in RPMI medium containing 10% FCS (RPMI + FCS) or in HBSS without amino acids and with low glucose levels (HBSS − FCS). At the indicated time points, specific transcript levels were quantified by qPCR and normalized to nonstarvation (RPMI + FCS) at time 2 h. Student's *t*-test was used to calculate significance between starved and nonstarved cells (∗, $p < 0.05$; ∗∗, $p < 0.01$; ∗∗∗, $p < 0.005$). In dependence on ATAXIN-2 deficiency ($n = 4$), (A) a significant downregulation of prion mRNA *PRNP* ($n = 4$), (B) a downregulation of citrate synthase mRNA *CS* ($n = 8$), and (C) a downregulation of the human GIS2 ortholog mRNA *CNBP* ($n = 6$) were observed.

factors like the prion protein RNQ1 and of molecular chaperones such as HSP12, HSP26, HSP104, HSP150, DDR48, SSA4, ATX1, PHB1, thus reducing the capacity of stress responses. RNQ1 [Rich in asparagine (N) and glutamine (Q) 1] is a yeast protein implicated in proteostasis pathways, which can adopt a toxic aggregation-prone prion conformation and modulates human polyglutamine aggregation toxicity.[57] These observations appear relevant, given that gain-of-function polyglutamine expansion mutations in ATXN2 result in prion-like protein aggregate formation and the sequestration of interacting proteins like the poly(A)-binding protein and the ubiquitin ligase PARK2 into the insoluble protein aggregates.[3,58] Thus, mutations in ATAXIN-2 modify the cellular capacity for stress responses, in particular the abundance of molecular chaperones and an aggregation-protein protein also in yeast.

However, both PBP1 and ATXN2 are localized at the rough endoplasmic reticulum in direct protein−protein interaction with poly(A)-binding protein and they cosediment with polysomes, while relocalizing to stress granules in times of low cellular energy.[5,6,26] They are never detectable in association with mitochondria, so how can they change the abundance of factors in the mitochondrial matrix in a selective manner?

It was therefore intriguing to observe a downregulation of GIS2 and of numerous GIS2-interactors in both PBP1 deletion strains, particularly under heat stress. GIS2 appears to be normally present in actively translating polysomes, similar to PBP1. In periods of cellular stress, it relocalizes together with PABPC1 and eIF4G to stress-induced RNP granules such as SG and PB, again similar to PBP1.[59−61] Interestingly, GIS2 acts as suppressor gene of the glucose/galactose growth defects of SNF1 mutants (*snf1 mig1 srb8/10/11*) and is known to rescue states of dNTP depletion that occur in parallel to AMP accumulation, again in analogy to PBP1, which is known to be downstream of SNF1, the yeast ortholog of human AMP kinase.[12,62,63]

Beyond these similarities, it was recently discovered that both GIS2 and PBP1 have a role in the feedback between mitochondrial needs and the corresponding protein synthesis at the ribosomal translation apparatus. Studies were conducted of a dominant $AAC2^{A128P}$ adenine nucleotide translocase allele at the inner mitochondrial membrane, which causes protein misfolding and loss of the mitochondrial proton gradient with a subsequent reduction of mitochondrial protein precursor import and an accumulation of such precursors outside the import pore.[10] It was revealed that this mitochondrial precursor overaccumulation stress (mPOS) leads to the induction of GIS2 at the translation apparatus. The ensuing mitochondrially triggered cell death could be rescued in a genetic multicopy suppressor screen by upregulation of PBP1 and 30 more factors in the pathways ribosome/translation, tRNA methylation, mRNA turnover/silencing, protein chaperoning/degradation, and mTOR signaling. The authors argued that a reduction in the synthesis rate of mitochondrial precursor proteins is crucial to minimize the cytosolic proteostatic stress that results from mitochondrial import failure. They also stated that this crosstalk between mitochondria and ribosomal translation

DOI: 10.1021/acs.jproteome.6b00647
J. Proteome Res. 2017, 16, 504−515

must be particularly important for neurons with their high mitochondrial density and for neurodegenerative disease.[10] While this publication studied a mutation of a mitochondrial inner membrane protein and documented responses and modifiers at the ribosomal translation apparatus, our manuscript studies a mutation of the translation modifier PBP1 and documents selective responses of enzymes in the mitochondrial matrix, providing nice complementary evidence of this novel feedback between mitochondria and the cytosolic synthesis of nuclear-encoded proteins destined to mitochondria. The novel concept of mitochondrial precursor overaccumulation stress is supported by our data.

The human ortholog of GIS2 is known as CNBP (Cellular Nucleic Acid Binding Protein) or ZNF9 (zink finger protein 9). Dominant mutations in the corresponding gene cause Myotonic Dystrophy type 2 (DM2 or PROMM), a disorder that is caused by an unstable DNA repeat expansion and has progressive external ophthalmoplegia similar to the Spinocerebellar Ataxia type 2 that is triggered by ATXN2-mutations, while DM2 pathogenesis is characterized by impaired RNA processing and global protein turnover.[64] Given that GIS2/CNBP acts as translational cap-independent activator for mRNAs with internal ribosome entry sites during periods of cellular stress, while reducing the abundance of ribosome assembly factors,[59−61] it appears to be crucial for the suppression of global protein synthesis in parallel to the induction of repair factors. It will be worthwhile to test if PBP1/ATXN2 interact with GIS2/CNBP as proteins directly or indirectly via common RNA targets, or if they interact genetically and mutually rescue the mutant phenotypes.

In contrast to the substantial effects on the abundance of enzymes in the cytosolic bioenergetics and mitochondrial metabolism, there was no significant change in the best established PBP1 interactor, the poly(A)-binding protein PAB1, and other interactors of the translation initiation complex. This is consistent with observations in mammals, where ATXN2 mutations result in only subtle alterations of PABPC1 levels.[3,4,31]

A mildly significant enrichment was noted for eisosome factors during cell stress. Although this is a pathway with only seven components and its statistical power is obviously limited, the factors EIS1, LSP1, PIL1, and YGR130C were all downregulated by both stressors in the SM strain. Eisosomes mark static sites for the endocytosis of lipid and peptide cargoes, independent from clathrin-mediated endocytosis.[65,66] Although the dysregulated eisosome factors do not have obvious sequence-homologues in mammalian cells, it is interesting to note that ATXN2 interacts with endophilin-A proteins at the plasma membranes,[27,28] which are crucial for a fast-acting clathrin-independent endocytosis at the leading edge of cell growth, which is thought to be responsible for the internalization of micronutrients and the turnover of membrane lipids.[67,68] Proline-rich motifs in ATXN2 and SH3 domains in endophilin-A mediate their interaction, and indeed the proline-rich motifs are conserved among the orthologs of ATXN2 until yeast and plants,[69,70] with strong effects on cellular endocytosis and growth signaling in mammals.[27,29,54]

CONCLUSION

Overall, PBP1 deletion in the absence of stress has a selective impact on cytoplasmic bioenergetics, mitochondrial metabolism, and the stress response capacity. During stress periods, these effects become more pronounced and widespread, and particularly a downregulation on the SG component GIS2 indicates an impact on the feedback between mitochondrial needs and cytoplasmic precursor protein synthesis, a novel concept named mPOS (mitochondrial precursor overaccumulation stress).[10] A plausible scenario of the roles of PBP1/ATXN2 would comprise its actions at the rER translation machinery to protect the stability of specific mRNAs while retaining them at stress granules in periods of low energy and cell damage to ensure their repair. This would explain why PBP1/ATXN2 ablation could reduce stress granule formation and why conversely its overexpression can diminish the RNA decay at P-bodies.[31] PBP1/ATXN2 would bind preferentially to mRNAs encoding for cytosolic bioenergetics and mitochondrial metabolism enzymes that may alleviate the starvation in stress periods as well as mRNAs encoding molecular chaperones that are needed for repair after cell stress. During mitochondrial dysfunction and mPOS, the immobilization of specific mRNAs at stress granules may reduce the load of mitochondrial precursor proteins being synthesized. The interaction of PBP1/ATXN2 with these selected mRNAs would be at their 3′ UTR in association with poly(A)-binding protein and would influence their translation rate, their poly(A)-tail length, and their turnover, probably via the CCR4/NOT complex. In parallel, PBP1/ATXN2 may undergo protein−protein interactions with the machinery of micronutrient endocytosis, may sequestrate growth kinases such as mTORC1, and associate with nuclear transcription factors to adapt the cell to the metabolic needs of stress periods. These novel insights may become useful for neuroprotective therapies in spinocerebellar ataxias, motor neuron diseases such as amyotrophic lateral sclerosis, and Parkinson's disease. Given that the gene locus of ATXN2 in man is also associated with diabetes mellitus type 1 and hypertension, the data may also elucidate bioenergetics regulations that underlie the human metabolic syndrome.

ASSOCIATED CONTENT

Supporting Information

The Supporting Information is available free of charge on the ACS Publications website at DOI: 10.1021/acs.jproteome.6b00647.

Original MaxQuant output files of all identified protein groups including LFQ intensities, sequence coverage, and PEP (XLSX)

Specific comparisons of strains and stress conditions, as indicated on individual sheets, using only valid values (XLSX)

Pearson correlation between SM, DB, and BY strains without stress and the two stress conditions heat and NaN_3 in scatter plots, indicating biological replicates (PDF)

SI table of contents (PDF)

AUTHOR INFORMATION

Corresponding Author

*E-mail: auburger@em.uni-frankfurt.de. Phone +49-69-6301-7428.

ORCID

David Meierhofer: 0000-0002-0170-868X

Author Contributions

§These authors share joint first authorship of this work.

DOI: 10.1021/acs.jproteome.6b00647
J. Proteome Res. 2017, 16, 504−515

Author Contributions

⊥These authors share joint senior authorship of this work.

Notes

The authors declare no competing financial interest.

■ ACKNOWLEDGMENTS

We are grateful to B. Meseck Selchow and Beata Lukazewska-McGreal for technical assistance. The project was financially supported by the DFG (AU96/11-3 and KR1949/3-1) and the Max Planck Society.

■ ABBREVIATIONS

BH, Benjamini−Hochberg; BY, strain BY4741 (MATa; ura3Δ0; leu2Δ0; his3Δ1; met15Δ0); DB, ΔPBP1-deletion strain; from EUROSCARF, ΔPBP1-deletion bank; FDR, false discovery rate; GO, Gene Ontology; GSEA, gene set enrichment analysis; HILIC, hydrophilic interaction chromatography; KEGG, Kyoto Encyclopedia of Genes and Genomes; LFQ, label-free quantification; PEP, posterior error probability; PPI, protein−protein interaction; RP, reversed phase; SG, stress granules; SM, ΔPBP1-deletion strain; self-made

■ REFERENCES

(1) Mangus, D. A.; Amrani, N.; Jacobson, A. Pbp1p, a factor interacting with Saccharomyces cerevisiae poly(A)-binding protein, regulates polyadenylation. *Mol. Cell. Biol.* **1998**, *18* (12), 7383−7396.

(2) Kozlov, G.; Safaee, N.; Rosenauer, A.; Gehring, K. Structural basis of binding of P-body-associated proteins GW182 and ataxin-2 by the Mlle domain of poly(A)-binding protein. *J. Biol. Chem.* **2010**, *285* (18), 13599−13606.

(3) Damrath, E.; Heck, M. V.; Gispert, S.; Azizov, M.; Nowock, J.; Seifried, C.; Rub, U.; Walter, M.; Auburger, G. ATXN2-CAG42 sequesters PABPC1 into insolubility and induces FBXW8 in cerebellum of old ataxic knock-in mice. *PLoS Genet.* **2012**, *8* (8), e1002920.

(4) Fittschen, M.; Lastres-Becker, I.; Halbach, M. V.; Damrath, E.; Gispert, S.; Azizov, M.; Walter, M.; Muller, S.; Auburger, G. Genetic ablation of ataxin-2 increases several global translation factors in their transcript abundance but decreases translation rate. *Neurogenetics* **2015**, *16* (3), 181−192.

(5) Satterfield, T. F.; Pallanck, L. J. Ataxin-2 and its Drosophila homolog, ATX2, physically assemble with polyribosomes. *Hum. Mol. Genet.* **2006**, *15* (16), 2523−2532.

(6) Ralser, M.; Albrecht, M.; Nonhoff, U.; Lengauer, T.; Lehrach, H.; Krobitsch, S. An integrative approach to gain insights into the cellular function of human ataxin-2. *J. Mol. Biol.* **2005**, *346* (1), 203−214.

(7) Kimura, Y.; Irie, K. Pbp1 is involved in Ccr4- and Khd1-mediated regulation of cell growth through association with ribosomal proteins Rpl12a and Rpl12b. *Eukaryotic Cell* **2013**, *12* (6), 864−874.

(8) Salvi, J. S.; Chan, J. N.; Szafranski, K.; Liu, T. T.; Wu, J. D.; Olsen, J. B.; Khanam, N.; Poon, B. P.; Emili, A.; Mekhail, K. Roles for Pbp1 and caloric restriction in genome and lifespan maintenance via suppression of RNA-DNA hybrids. *Dev. Cell* **2014**, *30* (2), 177−191.

(9) Dunn, C. D.; Jensen, R. E. Suppression of a defect in mitochondrial protein import identifies cytosolic proteins required for viability of yeast cells lacking mitochondrial DNA. *Genetics* **2003**, *165* (1), 35−45.

(10) Wang, X.; Chen, X. J. A cytosolic network suppressing mitochondria-mediated proteostatic stress and cell death. *Nature* **2015**, *524* (7566), 481−484.

(11) Takahara, T.; Maeda, T. Transient sequestration of TORC1 into stress granules during heat stress. *Mol. Cell* **2012**, *47* (2), 242−252.

(12) DeMille, D.; Badal, B. D.; Evans, J. B.; Mathis, A. D.; Anderson, J. F.; Grose, J. H. PAS kinase is activated by direct SNF1-dependent phosphorylation and mediates inhibition of TORC1 through the phosphorylation and activation of Pbp1. *Molecular biology of the cell* **2015**, *26* (3), 569−582.

(13) Swisher, K. D.; Parker, R. Localization to, and effects of Pbp1, Pbp4, Lsm12, Dhh1, and Pab1 on stress granules in Saccharomyces cerevisiae. *PLoS One* **2010**, *5* (4), e10006.

(14) Mangus, D. A.; Smith, M. M.; McSweeney, J. M.; Jacobson, A. Identification of factors regulating poly(A) tail synthesis and maturation. *Molecular and cellular biology* **2004**, *24* (10), 4196−4206.

(15) Tadauchi, T.; Inada, T.; Matsumoto, K.; Irie, K. Posttranscriptional regulation of HO expression by the Mkt1-Pbp1 complex. *Molecular and cellular biology* **2004**, *24* (9), 3670−3681.

(16) Elden, A. C.; Kim, H. J.; Hart, M. P.; Chen-Plotkin, A. S.; Johnson, B. S.; Fang, X.; Armakola, M.; Geser, F.; Greene, R.; Lu, M. M.; Padmanabhan, A.; Clay-Falcone, D.; McCluskey, L.; Elman, L.; Juhr, D.; Gruber, P. J.; Rub, U.; Auburger, G.; Trojanowski, J. Q.; Lee, V. M.; Van Deerlin, V. M.; Bonini, N. M.; Gitler, A. D. Ataxin-2 intermediate-length polyglutamine expansions are associated with increased risk for ALS. *Nature* **2010**, *466* (7310), 1069−1075.

(17) Colombrita, C.; Zennaro, E.; Fallini, C.; Weber, M.; Sommacal, A.; Buratti, E.; Silani, V.; Ratti, A. TDP-43 is recruited to stress granules in conditions of oxidative insult. *J. Neurochem.* **2009**, *111* (4), 1051−1061.

(18) Aulas, A.; Caron, G.; Gkogkas, C. G.; Mohamed, N. V.; Destroismaisons, L.; Sonenberg, N.; Leclerc, N.; Parker, J. A.; Vande Velde, C. G3BP1 promotes stress-induced RNA granule interactions to preserve polyadenylated mRNA. *J. Cell Biol.* **2015**, *209* (1), 73−84.

(19) Ling, J. P.; Pletnikova, O.; Troncoso, J. C.; Wong, P. C. NEURODEGENERATION. TDP-43 repression of nonconserved cryptic exons is compromised in ALS-FTD. *Science* **2015**, *349* (6248), 650−655.

(20) Al-Ramahi, I.; Perez, A. M.; Lim, J.; Zhang, M.; Sorensen, R.; de Haro, M.; Branco, J.; Pulst, S. M.; Zoghbi, H. Y.; Botas, J. dAtaxin-2 mediates expanded Ataxin-1-induced neurodegeneration in a Drosophila model of SCA1. *PLoS Genet.* **2007**, *3* (12), e234.

(21) Shulman, J. M.; Feany, M. B. Genetic modifiers of tauopathy in Drosophila. *Genetics* **2003**, *165* (3), 1233−1242.

(22) Ghosh, S.; Feany, M. B. Comparison of pathways controlling toxicity in the eye and brain in Drosophila models of human neurodegenerative diseases. *Human molecular genetics* **2004**, *13* (18), 2011−2018.

(23) Khurana, V.; Lu, Y.; Steinhilb, M. L.; Oldham, S.; Shulman, J. M.; Feany, M. B. TOR-mediated cell-cycle activation causes neurodegeneration in a Drosophila tauopathy model. *Curr. Biol.* **2006**, *16* (3), 230−241.

(24) Lessing, D.; Bonini, N. M. Polyglutamine genes interact to modulate the severity and progression of neurodegeneration in Drosophila. *PLoS Biol.* **2008**, *6* (2), e29.

(25) Na, D.; Rouf, M.; O'Kane, C. J.; Rubinsztein, D. C.; Gsponer, J. NeuroGeM, a knowledgebase of genetic modifiers in neurodegenerative diseases. *BMC Med. Genomics* **2013**, *6*, 52.

(26) van de Loo, S.; Eich, F.; Nonis, D.; Auburger, G.; Nowock, J. Ataxin-2 associates with rough endoplasmic reticulum. *Exp. Neurol.* **2009**, *215* (1), 110−118.

(27) Nonis, D.; Schmidt, M. H.; van de Loo, S.; Eich, F.; Dikic, I.; Nowock, J.; Auburger, G. Ataxin-2 associates with the endocytosis complex and affects EGF receptor trafficking. *Cell. Signalling* **2008**, *20* (10), 1725−1739.

(28) Ralser, M.; Nonhoff, U.; Albrecht, M.; Lengauer, T.; Wanker, E. E.; Lehrach, H.; Krobitsch, S. Ataxin-2 and huntingtin interact with endophilin-A complexes to function in plastin-associated pathways. *Hum. Mol. Genet.* **2005**, *14* (19), 2893−2909.

(29) Drost, J.; Nonis, D.; Eich, F.; Leske, O.; Damrath, E.; Brunt, E. R.; Lastres-Becker, I.; Heumann, R.; Nowock, J.; Auburger, G. Ataxin-2 modulates the levels of Grb2 and SRC but not ras signaling. *J. Mol. Neurosci.* **2013**, *51* (1), 68−81.

(30) Auburger, G.; Gispert, S.; Lahut, S.; Omur, O.; Damrath, E.; Heck, M.; Basak, N. 12q24 locus association with type 1 diabetes: SH2B3 or ATXN2? *World journal of diabetes* **2014**, *5* (3), 316−327.

DOI: 10.1021/acs.jproteome.6b00647
J. Proteome Res. 2017, 16, 504−515

(31) Nonhoff, U.; Ralser, M.; Welzel, F.; Piccini, I.; Balzereit, D.; Yaspo, M. L.; Lehrach, H.; Krobitsch, S. Ataxin-2 interacts with the DEAD/H-box RNA helicase DDX6 and interferes with P-bodies and stress granules. *Molecular biology of the cell* **2007**, *18* (4), 1385−1396.
(32) Lastres-Becker, I.; Brodesser, S.; Lutjohann, D.; Azizov, M.; Buchmann, J.; Hintermann, E.; Sandhoff, K.; Schurmann, A.; Nowock, J.; Auburger, G. Insulin receptor and lipid metabolism pathology in ataxin-2 knock-out mice. *Hum. Mol. Genet.* **2008**, *17* (10), 1465−1481.
(33) Aretz, I.; Hardt, C.; Wittig, I.; Meierhofer, D. An Impaired Respiratory Electron Chain Triggers Down-regulation of the Energy Metabolism and De-ubiquitination of Solute Carrier Amino Acid Transporters. *Mol. Cell. Proteomics* **2016**, *15* (5), 1526−1538.
(34) Halbach, M. V.; Gispert, S.; Stehning, T.; Damrath, E.; Walter, M.; Auburger, G. Atxn2 Knockout and CAG42-Knock-in Cerebellum Shows Similarly Dysregulated Expression in Calcium Homeostasis Pathway. *Cerebellum* **2016**. DOI: 10.1007/s12311-016-0762-4.
(35) Meier, I. D.; Bernreuther, C.; Tilling, T.; Neidhardt, J.; Wong, Y. W.; Schulze, C.; Streichert, T.; Schachner, M. Short DNA sequences inserted for gene targeting can accidentally interfere with off-target gene expression. *FASEB J.* **2010**, *24* (6), 1714−1724.
(36) Buchan, J. R.; Yoon, J. H.; Parker, R. Stress-specific composition, assembly and kinetics of stress granules in Saccharomyces cerevisiae. *J. Cell Sci.* **2011**, *124* (2), 228−239.
(37) McNaughton, D.; Knight, W.; Guerreiro, R.; Ryan, N.; Lowe, J.; Poulter, M.; Nicholl, D. J.; Hardy, J.; Revesz, T.; Rossor, M.; Collinge, J.; Mead, S.; Lowe, J. Duplication of amyloid precursor protein (APP), but not prion protein (PRNP) gene is a significant cause of early onset dementia in a large UK series. *Neurobiol. Aging* **2012**, *33* (2), 426.e13−426.e21.
(38) Kara, E.; Kiely, A. P.; Proukakis, C.; Giffin, N.; Love, S.; Hehir, J.; Rantell, K.; Pandraud, A.; Hernandez, D. G.; Nacheva, E.; Pittman, A. M.; Nalls, M. A.; Singleton, A. B.; Revesz, T.; Bhatia, K. P.; Quinn, N.; Hardy, J.; Holton, J. L.; Houlden, H. A 6.4 Mb duplication of the alpha-synuclein locus causing frontotemporal dementia and Parkinsonism: phenotype-genotype correlations. *JAMA neurology* **2014**, *71* (9), 1162−1171.
(39) Royston, M. C.; Mann, D.; Pickering-Brown, S.; Owen, F.; Perry, R.; Ragbhavan, R.; Khin-Nu, C.; Tyner, S.; Day, K.; Crook, R.; Hardy, J.; Roberts, G. W. ApoE2 allele, Down's syndrome, and dementia. *Ann. N. Y. Acad. Sci.* **1996**, *777*, 255−259.
(40) Baker Brachmann, C.; Davies, A.; Cost, G. J.; Caputo, E.; Li, J.; Hieter, P.; Boeke, J. D. Designer deletion strains derived from Saccharomyces cerevisiae S288C: a useful set of strains and plasmids for PCR-mediated gene disruption and other applications. *Yeast* **1998**, *14* (2), 115−132.
(41) Winzeler, E. A.; Shoemaker, D. D.; Astromoff, A.; Liang, H.; Anderson, K.; Andre, B.; Bangham, R.; Benito, R.; Boeke, J. D.; Bussey, H.; Chu, A. M.; Connelly, C.; Davis, K.; Dietrich, F.; Dow, S. W.; El Bakkoury, M.; Foury, F.; Friend, S. H.; Gentalen, E.; Giaever, G.; Hegemann, J. H.; Jones, T.; Laub, M.; Liao, H.; Liebundguth, N.; Lockhart, D. J.; Lucau-Danila, A.; Lussier, M.; M'Rabet, N.; Menard, P.; Mittmann, M.; Pai, C.; Rebischung, C.; Revuelta, J. L.; Riles, L.; Roberts, C. J.; Ross-MacDonald, P.; Scherens, B.; Snyder, M.; Sookhai-Mahadeo, S.; Storms, R. K.; Veronneau, S.; Voet, M.; Volckaert, G.; Ward, T. R.; Wysocki, R.; Yen, G. S.; Yu, K.; Zimmermann, K.; Philippsen, P.; Johnston, M.; Davis, R. W. Functional characterization of the S. cerevisiae genome by gene deletion and parallel analysis. *Science* **1999**, *285* (5429), 901−906.
(42) Guldener, U.; Heck, S.; Fielder, T.; Beinhauer, J.; Hegemann, J. H. A new efficient gene disruption cassette for repeated use in budding yeast. *Nucleic acids research* **1996**, *24* (13), 2519−2524.
(43) Grousl, T.; Ivanov, P.; Malcova, I.; Pompach, P.; Frydlova, I.; Slaba, R.; Senohrabkova, L.; Novakova, L.; Hasek, J. Heat shock-induced accumulation of translation elongation and termination factors precedes assembly of stress granules in S. cerevisiae. *PLoS One* **2013**, *8* (2), e57083.
(44) Hebert, A. S.; Richards, A. L.; Bailey, D. J.; Ulbrich, A.; Coughlin, E. E.; Westphall, M. S.; Coon, J. J. The one hour yeast proteome. *Mol. Cell. Proteomics* **2014**, *13* (1), 339−347.
(45) Tyanova, S.; Mann, M.; Cox, J. MaxQuant for in-depth analysis of large SILAC datasets. *Methods Mol. Biol.* **2014**, *1188*, 351−364.
(46) Cox, J.; Neuhauser, N.; Michalski, A.; Scheltema, R. A.; Olsen, J. V.; Mann, M. Andromeda: a peptide search engine integrated into the MaxQuant environment. *J. Proteome Res.* **2011**, *10* (4), 1794−1805.
(47) Vizcaino, J. A.; Cote, R. G.; Csordas, A.; Dianes, J. A.; Fabregat, A.; Foster, J. M.; Griss, J.; Alpi, E.; Birim, M.; Contell, J.; O'Kelly, G.; Schoenegger, A.; Ovelleiro, D.; Perez-Riverol, Y.; Reisinger, F.; Rios, D.; Wang, R.; Hermjakob, H. The PRoteomics IDEntifications (PRIDE) database and associated tools: status in 2013. *Nucleic Acids Res.* **2013**, *41* (D1), D1063−D1069.
(48) Franceschini, A.; Szklarczyk, D.; Frankild, S.; Kuhn, M.; Simonovic, M.; Roth, A.; Lin, J.; Minguez, P.; Bork, P.; von Mering, C.; Jensen, L. J. STRING v9.1: protein-protein interaction networks, with increased coverage and integration. *Nucleic Acids Res.* **2013**, *41* (D1), D808−D815.
(49) Sen, N. E.; Drost, J.; Gispert, S.; Torres-Odio, S.; Damrath, E.; Klinkenberg, M.; Hamzeiy, H.; Akdal, G.; Gulluoglu, H.; Basak, A. N.; Auburger, G. Search for SCA2 blood RNA biomarkers highlights Ataxin-2 as strong modifier of the mitochondrial factor PINK1 levels. *Neurobiol. Dis.* **2016**, *96*, 115−126.
(50) Livak, K. J.; Schmittgen, T. D. Analysis of relative gene expression data using real-time quantitative PCR and the 2(-Delta Delta C(T)) Method. *Methods* **2001**, *25* (4), 402−408.
(51) Lai, L. C.; Kosorukoff, A. L.; Burke, P. V.; Kwast, K. E. Dynamical remodeling of the transcriptome during short-term anaerobiosis in Saccharomyces cerevisiae: differential response and role of Msn2 and/or Msn4 and other factors in galactose and glucose media. *Molecular and cellular biology* **2005**, *25* (10), 4075−4091.
(52) Meierhofer, D.; Halbach, M.; Sen, N. E.; Gispert, S.; Auburger, G. Atxn2-Knock-Out mice show branched chain amino acids and fatty acids pathway alterations. *Mol. Cell. Proteomics* **2016**, *15*, 1728.
(53) Bar, D. Z.; Charar, C.; Dorfman, J.; Yadid, T.; Tafforeau, L.; Lafontaine, D. L.; Gruenbaum, Y. Cell size and fat content of dietary-restricted Caenorhabditis elegans are regulated by ATX-2, an mTOR repressor. *Proc. Natl. Acad. Sci. U. S. A.* **2016**, *113* (32), E4620−4629.
(54) Lastres-Becker, I.; Nonis, D.; Eich, F.; Klinkenberg, M.; Gorospe, M.; Kotter, P.; Klein, F. A.; Kedersha, N.; Auburger, G. Mammalian ataxin-2 modulates translation control at the pre-initiation complex via PI3K/mTOR and is induced by starvation. *Biochim. Biophys. Acta, Mol. Basis Dis.* **2016**, *1862* (9), 1558−1569.
(55) Klinkenberg, M.; Gispert, S.; Dominguez-Bautista, J. A.; Braun, I.; Auburger, G.; Jendrach, M. Restriction of trophic factors and nutrients induces PARKIN expression. *Neurogenetics* **2012**, *13* (1), 9−21.
(56) Parganlija, D.; Klinkenberg, M.; Dominguez-Bautista, J.; Hetzel, M.; Gispert, S.; Chimi, M. A.; Drose, S.; Mai, S.; Brandt, U.; Auburger, G.; Jendrach, M. Loss of PINK1 impairs stress-induced autophagy and cell survival. *PLoS One* **2014**, *9* (4), e95288.
(57) Duennwald, M. L.; Jagadish, S.; Giorgini, F.; Muchowski, P. J.; Lindquist, S. A network of protein interactions determines polyglutamine toxicity. *Proc. Natl. Acad. Sci. U. S. A.* **2006**, *103* (29), 11051−11056.
(58) Halbach, M. V.; Stehning, T.; Damrath, E.; Jendrach, M.; Sen, N. E.; Basak, A. N.; Auburger, G. Both ubiquitin ligases FBXW8 and PARK2 are sequestrated into insolubility by ATXN2 PolyQ expansions, but only FBXW8 expression is dysregulated. *PLoS One* **2015**, *10* (3), e0121089.
(59) Sammons, M. A.; Samir, P.; Link, A. J. Saccharomyces cerevisiae Gis2 interacts with the translation machinery and is orthogonal to myotonic dystrophy type 2 protein ZNF9. *Biochem. Biophys. Res. Commun.* **2011**, *406* (1), 13−19.
(60) Rojas, M.; Farr, G. W.; Fernandez, C. F.; Lauden, L.; McCormack, J. C.; Wolin, S. L. Yeast Gis2 and its human ortholog CNBP are novel components of stress-induced RNP granules. *PLoS One* **2012**, *7* (12), e52824.
(61) Scherrer, T.; Femmer, C.; Schiess, R.; Aebersold, R.; Gerber, A. P. Defining potentially conserved RNA regulons of homologous zinc-finger RNA-binding proteins. *Genome biology* **2011**, *12* (1), R3.

DOI: 10.1021/acs.jproteome.6b00647
J. Proteome Res. 2017, 16, 504−515

(62) Balciunas, D.; Ronne, H. Yeast genes GIS1−4: multicopy suppressors of the Gal- phenotype of snf1 mig1 srb8/10/11 cells. *Mol. Gen. Genet.* **1999**, *262* (4−5), 589−599.
(63) Earp, C.; Rowbotham, S.; Merenyi, G.; Chabes, A.; Cha, R. S. S phase block following MEC1ATR inactivation occurs without severe dNTP depletion. *Biol. Open* **2015**, *4* (12), 1739−1743.
(64) Meola, G.; Jones, K.; Wei, C.; Timchenko, L. T. Dysfunction of protein homeostasis in myotonic dystrophies. *Histology and histopathology* **2013**, *28* (9), 1089−1098.
(65) Walther, T. C.; Brickner, J. H.; Aguilar, P. S.; Bernales, S.; Pantoja, C.; Walter, P. Eisosomes mark static sites of endocytosis. *Nature* **2006**, *439* (7079), 998−1003.
(66) Michelot, A.; Costanzo, M.; Sarkeshik, A.; Boone, C.; Yates, J. R., 3rd; Drubin, D. G. Reconstitution and protein composition analysis of endocytic actin patches. *Curr. Biol.* **2010**, *20* (21), 1890−1899.
(67) Boucrot, E.; Ferreira, A. P.; Almeida-Souza, L.; Debard, S.; Vallis, Y.; Howard, G.; Bertot, L.; Sauvonnet, N.; McMahon, H. T. Endophilin marks and controls a clathrin-independent endocytic pathway. *Nature* **2014**, *517* (7535), 460−465.
(68) Renard, H. F.; Simunovic, M.; Lemiere, J.; Boucrot, E.; Garcia-Castillo, M. D.; Arumugam, S.; Chambon, V.; Lamaze, C.; Wunder, C.; Kenworthy, A. K.; Schmidt, A. A.; McMahon, H. T.; Sykes, C.; Bassereau, P.; Johannes, L. Endophilin-A2 functions in membrane scission in clathrin-independent endocytosis. *Nature* **2014**, *517* (7535), 493−496.
(69) Jimenez-Lopez, D.; Guzman, P. Insights into the evolution and domain structure of Ataxin-2 proteins across eukaryotes. *BMC Res. Notes* **2014**, *7*, 453.
(70) Jimenez-Lopez, D.; Bravo, J.; Guzman, P. Evolutionary history exposes radical diversification among classes of interaction partners of the MLLE domain of plant poly(A)-binding proteins. *BMC Evol. Biol.* **2015**, *15*, 195.

NOTE ADDED AFTER ASAP PUBLICATION

A partially corrected version of this paper was published on December 22, 2016. The fully corrected version was re-posted on December 27, 2016.

DOI: 10.1021/acs.jproteome.6b00647
J. Proteome Res. 2017, 16, 504−515